Wind and Structures, *Vol. 22, No. 4 (2016) 409-428*
DOI: http://dx.doi.org/10.12989/was.2016.22.4.409

Systematic influence of wind incident directions on wind circulation in the re-entrant corners of high-rise buildings

Qureshi M. Zahid Iqbal[*1] and A.L.S. Chan[2]

[1]*Department of Architecture and Civil Engineering, College of Science and Engineering, City University of Hong Kong, Hong Kong*
[2]*Division of Building Science and Technology, College of Science and Engineering, City University of Hong Kong, Hong Kong*

(Received December 3, 2015, Revised February 19, 2016, Accepted February 21, 2016)

Abstract. The mechanical and aerodynamic effect of building shape plays a dominate role in the pedestrian level wind environment. These effects have been presented in numerous studies and are available in many wind codes. However, most studies have focused on wind flow around conventional buildings and are limited to few wind directions. The present study investigated wind circulation in the re-entrant corners of cross-shaped high-rise buildings from various wind directions. The investigation focused on the pedestrian level wind environment in the re-entrant corners with different aspect ratios of building arrangements. Ninety cases of case study arrangements were evaluated using wind tunnel experimentation. The results show that for adequate wind circulation in the re-entrant corners, building orientations and separations play a critical role. Furthermore, in normal wind incident directions and at a high aspect ratio, poor wind flow was observed in the re-entrant corners. Moreover, it was noted that an optimized building orientation and aspect ratio significantly improved the wind flow in re-entrant corners and through passages. In addition, it was observed that oblique wind incident direction increased wind circulation in the re-entrant corners and through passages.

Keywords: wind tunnel experiment; re-entrant corner; wind circulation; wind incident direction

1. Introduction

Wind flow around buildings plays a critical role in wind comfort and contaminant dispersion. When several high-rise buildings are built in proximity, they produce wind blockage effects that are common in metropolitan cities such as Hong Kong (Hang *et al*. 2012, Zhang *et al*. 2015). Wind blockage is not suitable for appropriate air circulation, especially in a deep street canyon. Wind flow is presently a major concern for new urban design, especially of high-rise buildings (Blocken and Stathopoulos 2013, Yang *et al*. 2015). Trends of constructing irregularly shaped buildings are increasing. Construction of irregularly shaped buildings increases the concerns of wind environment assessments, because of various curves and corners involved in the design of irregularly shaped buildings. Irregularly shaped buildings are typically designed for aesthetic and adequate ventilation purposes. However, recessed cavities are inherently secluded in the

*Corresponding author, E-mail: muqureshi3-c@my.cityu.edu.hk

http://www.techno-press.org/?journal=was&subpage=8 ISSN: 1226-6116 (Print), 1598-6225 (Online)

downstream side and covered within the stable vortex and stagnation zones (Gomes *et al*. 2005, Wong and Lam 2013). To disperse these stagnation zones, appropriate building orientation and wind flow is required. Studies have shown that wind flow in a deep canyon at the pedestrian level is critical for human health and comfort (Gao *et al*. 2009). Various numerical and experimental techniques are used to assess wind flow at the pedestrian level. Wind environment assessments around buildings and of wind flow through urban areas have been well documented. Various authors, such as Stathopoulos (2006), have investigated wind flow at the pedestrian level around buildings. Blocken and Carmeliet (2004), Blocken (2014) and Blocken (2015) have provided details of pedestrian level wind flow assessments. Similarly, Tsang *et al*. (2012), Janssen *et al*. (2013) and Kubota *et al*. (2008) have investigated wind flow around various building arrangements by using numerical and experimental approaches. For irregular shape buildings, most researchers have focused on wind load and flow only concerning limited wind directions. For instance, Chow *et al*. (2002) investigated wind flow within a re-entrant bay at the middle level of a high-rise building. Wang *et al*. (2012) studied the flow distribution in the vicinity of a U-shaped building. Similarly, Cheng *et al*. (2011) examined the wind flow and pollution dispersion within a re-entrant bay of a high-rise building. Various researchers, such as Higson *et al*. (1996), have mentioned that wind flow and pollution dispersions are directly related to each other. Furthermore, wind flow characteristics substantially depend on the shape and arrangement of buildings. Similar work was performed by Santos *et al*. (2005).

Few studies have focused on wind flow around irregular shaped buildings. Most studies have focused on the wind load and wind flow around conventional buildings. In the present study, wind flow in the re-entrant corners of cross-shaped high-rise buildings at the pedestrian level was investigated. The Harmony Blocks, composed of cross-shaped buildings, each Block consist of four re-entrant corners. Harmony Block is a commonly used residential building block in densely populated Hong Kong. Recently, Gao *et al*. (2009), Yeung and Yu (2007) have discussed the airborne transmission of various infections in a densely populated area caused by a lack of wind flow. The aforementioned studies have emphasized the relevance of analyzing the wind flow in recessed areas such as re-entrant bays and corners. The aforementioned brief review highlighted the value of wind circulation in the re-entrant corners, which is instrumental for both wind comfort and contaminant dispersion. The present study investigated wind circulation in the re-entrant corners of cross-shaped high-rise buildings in different arrangements from 16 wind directions by using wind tunnel experiments. The remainder of this paper is organized as follows: The experimental setup and wind assessment criteria are discussed in Section 2; Section 3 presents the results and a discussion of case study arrangements; finally, conclusions are drawn in Section 4.

2. Methodology

2.1 Experimental setup

This study investigated commonly used cross-shaped residential building blocks, the Harmony Blocks in Hong Kong. The experiment was performed in a closed circuit, subsonic boundary layer wind tunnel facility at the City University of Hong Kong. The cross-section of the wind tunnel, velocity sensor arrangements on the test board are shown in Fig. 1. A detailed layout of the wind tunnel is shown in Fig. 2. The building models were mounted on a rotating table with a diameter of 2 m (Fig. 1(a)).

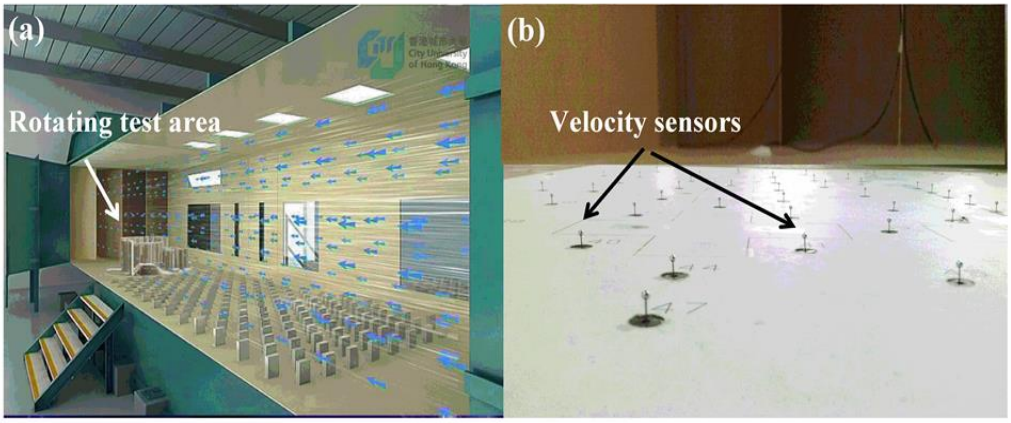

Fig. 1 Wind tunnel experiment (a) inside view of the boundary layer wind tunnel and (b) velocity sensors arrangement on the test board

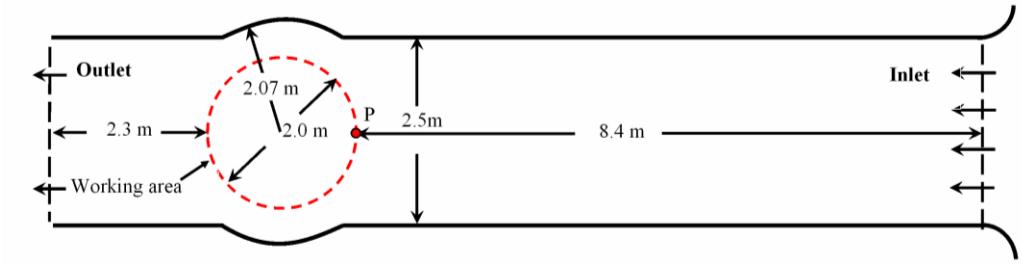

Fig. 2 Schematic of the boundary layer wind tunnel and test area (dotted circle)

The building models were fabricated using polystyrene at a scale of 1:280. The schematic arrangements of the building models are illustrated in Fig. 3. The maximum blockage ratio was 1.21%, which is less than the recommended blockage ratio of 3% (Franke *et al.* 2007, Tominaga *et al.* 2008). The test was conducted in three building separations (W). Each building consisted of four re-entrant corners, as shown in Fig. 3. Table 1 lists the four scenarios of building arrangements. In Configuration 1, eight buildings were arranged in a square shape. In Configurations 2, 3, and 4, seven, five, and three buildings were arranged in a U, L, and I shape respectively (Fig. 3).

Three building separations of 0.054 m, 0.107 m, and 0.142 m (15 m, 30 m, and 40 m, respectively, at a full scale) were investigated. For appropriate air ventilation, the Hong Kong Buildings Department recommends a minimum building separation of 15 m between high-rise buildings (Hong Kong Building Department). More building separations were investigated to study the influence of wind directions and building separations on the ventilation potential in the re-entrant corners. The small dots in Fig. 4 indicate the position of velocity sensors. Re-entrant corners are represented by C1 to C16. Passages are represented by P1 to P4. The building scale

height (H) was 0.4 m. The building scale dimensions S1, S2, and S3 were 0.048 m, 0.052 m, and 0.057 m, respectively (Fig. 4). Letters A to E were used to differentiate buildings.

To maintain the Reynolds number independency, Snyder (1972) mentioned that the Reynolds number should be maintained at a value greater than 4000. In the present study, Reynolds number independency was achieved by setting the reference wind speed (U_r) to 10 m/s at a height of 1.8 m within the wind tunnel of a height of 2 m.

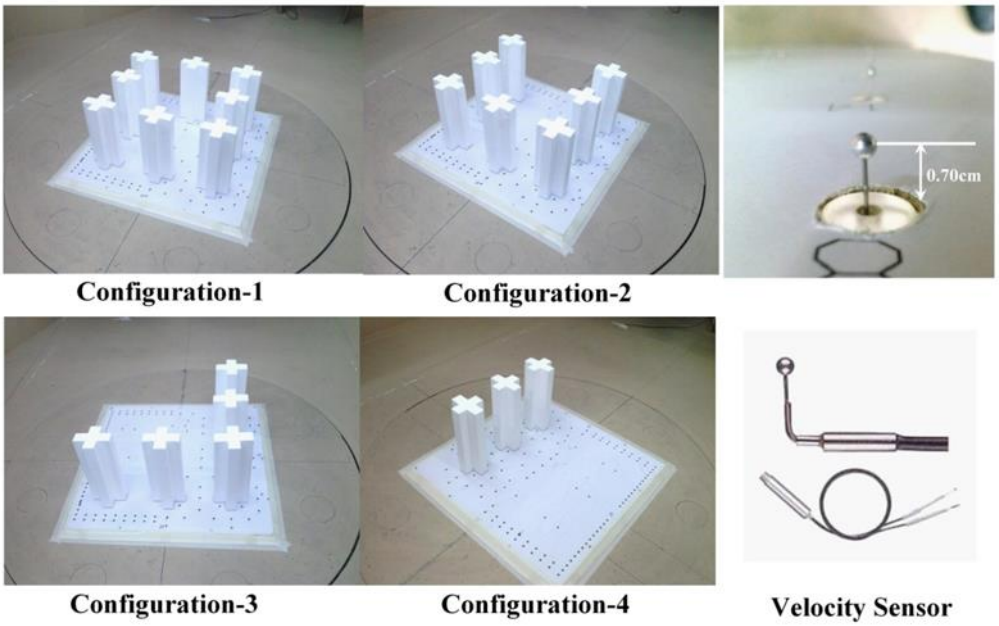

Fig. 3 Building model arrangements on test board and velocity sensor

Table 1 Test Cases

	Cases	Building separation W (m)
Configuration 1	Case 1	0.054
	Case 2	0.107
	Case 3	0.142
Configuration 2	Case 1	0.054
	Case 2	0.107
	Case 3	0.142
Configuration 3	Case 1	0.054
	Case 2	0.107
	Case 3	0.142
Configuration 4	Case 1	0.054
	Case 2	0.107
	Case 3	0.142

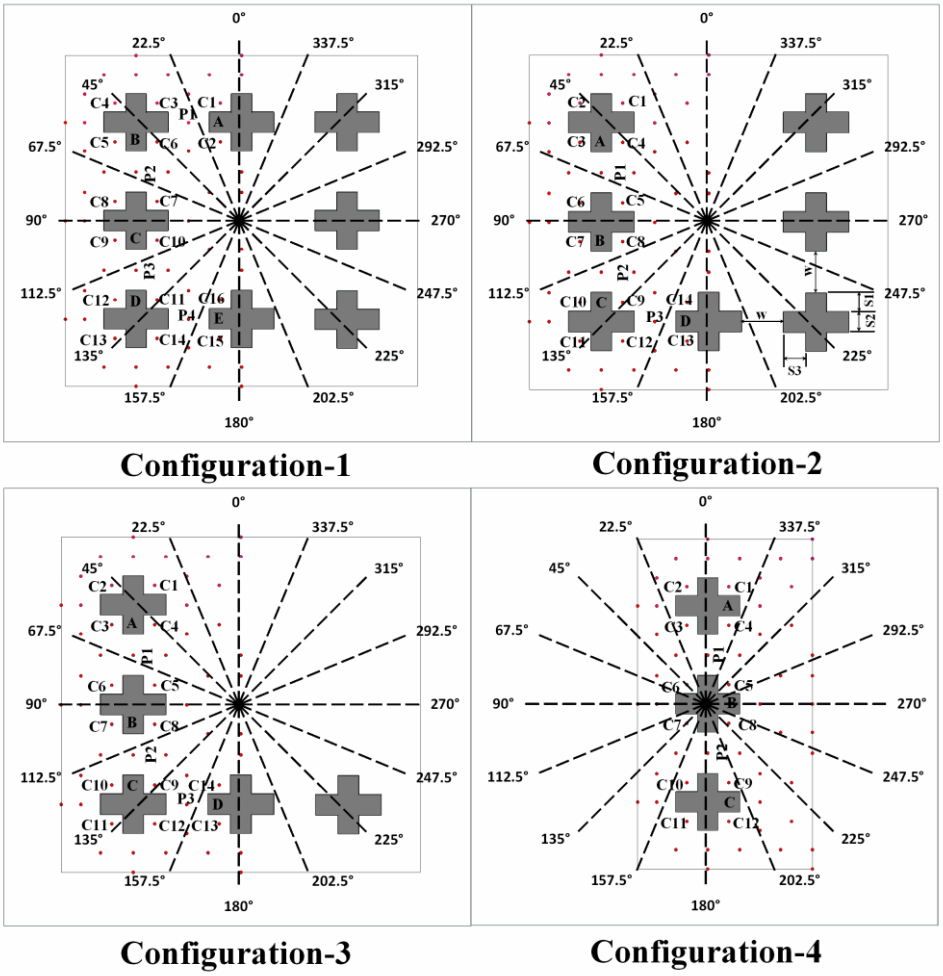

Fig. 4 Case study configurations and location of re-entrant corners and passages

Moreover, Reynolds number was set 1.1×10^5, according to the building height (H) and wind velocity at z=H, which is considerably greater than 4000. The flow was assumed to be horizontally homogeneous; therefore, wind and turbulent intensity profiles were measured at point 'P', as shown in Fig. 2. The wind velocity (U) was normalized by a reference wind speed. The profile of normalized wind speed (U/U_r) and the turbulent intensity profiles are provided in Fig. 5. The wind profile was set using a power law of exponent 0.15 that represents the open exposure terrain condition. The pedestrian level height of 0.007 m (2 m at a full scale) was considered for the analysis. The frontal area density varied from 0.06 to 0.18. A hotwire anemometer was used for the inlet and approaching wind profiles. Velocity sensors were arranged on the half-side of the test board because of the symmetric arrangements of the buildings. A total of 60 velocity sensors for Configurations 1, 2, and 3 as well as 48 velocity sensors for Configuration 4 were used with a multichannel measurement system to measure the velocity at numerous points simultaneously. In

this study, a Kanomax miniature L-shape velocity probe with a multichannel measuring system was used (Kanomax USA). The precision of each velocity sensor was ± 3%. The sampling time was 40 s with a frequency of 10 Hz. In all cases, the aspect ratio (H/W) was greater than 2. Previous studies have considered buildings with an aspect ratio greater than 2 to be a deep street canyon (Afiq *et al*. 2012). Thus, suitable natural ventilation is necessary at the pedestrian level for wind comfort and contaminant dispersion.

2.2 Wind evaluation criteria

At present, various wind assessment criteria are available for the wind tunnel investigation of wind environments. For instance, Stathopoulos *et al*. (1992) proposed an over speed ratio called an amplification factor (Eq. (1)) for the evaluation of wind flow at a particular point or location

$$k = \frac{U}{U_B} \tag{1}$$

where, k is the over speed ratio, and U and U_B are the wind velocities with and without the presence of a building at the same location, respectively. In another study, Ng (2009) investigated the pedestrian level wind flow for the case study area of Hong Kong. Ng (2009) used normalized wind velocity for the wind assessments and to propose guidelines. The Ng (2009) study was based on Hong Kong; therefore, the Ng (2009) wind assessment criterion was used in this study. Ng (2009) mentioned that for a comfortable wind environment, a wind speed of 1.0–1.5 m/s is required at the pedestrian level of a 2 m height. In Hong Kong, at 500 m, the mean wind speed is 6–8 m/s. Ng (2009) also reported normalized wind speeds of approximately 0.3 m/s and less than 0.3 m/s in open areas and congested areas, respectively. Therefore, wind at the pedestrian level (0.007 m) was normalized with the wind speed at a height of 1.8 m in the wind tunnel. Based on the Ng (2009) studies, normalized wind speed was categorized into three wind speed regions, as shown in Table 2. In this study, the wind environment in the re-entrant corners and flow through the passages were evaluated using the criteria defined in Table 2.

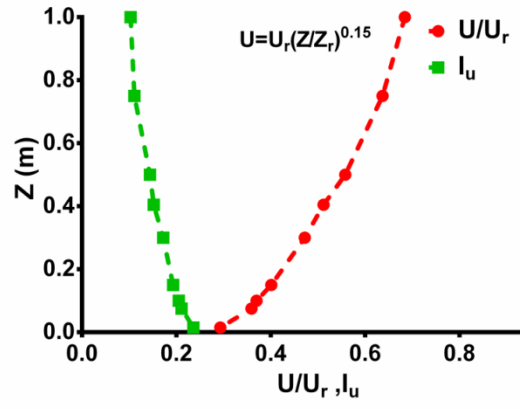

Fig. 5 Wind speed (U) and turbulent intensity profiles (I_u)

Table 2 Normalized wind speed regions

	Wind speed regions	U/U_r
1	Low wind speed region (L)	$U/U_r \leq 0.1$
2	Moderate wind speed region (M)	$0.1 < U/U_r \leq 0.3$
3	High wind speed region (H)	$U/U_r > 0.3$

3. Results and discussion

3.1 Acceleration and deceleration of wind flow in the re-entrant corners

This section details the acceleration and deceleration of wind flow in the re-entrant corners according to the normalized wind velocity ratio (WVR), as defined in Table 2.

3.1.1 Configuration 1

In this configuration, five wind directions (α) and 16 re-entrant corners were evaluated. Fig. 6 illustrates the distribution of the WVR in the re-entrant corners from five wind directions. Dotted lines separate the wind speed regions in Fig. 6, as illustrated in Table 2. At α = 0°, in Case 3, the WVR in C1 was higher than that in Case 1 and 2. In Case 1 and 2, at the same angle, because of the upstream wake generated at the entrance of P1, the WVR decreased. However, in Case 3, the passage width was more than that in Case 1. This reduced the effect of the stagnation zone within the wake in P1. In Case 3, the WVR in C1 was high because of the aerodynamic effects of the corners of Building A on the windward side. In C2, the WVR was almost equal in Case 3 and was reduced in Case 1 and 2 because of the downstream wake and venturi effect of the passage. From C4 to C16, the WVR was almost equal in all the cases, because of the normal wind directions and wake of the upstream buildings.

At α = 22.5°, WVR variations were similar to those at α = 0°. At α = 45°, all re-entrant corners were in Regions A and H, except C15, which was in a low wind speed (L) region. Similarly, re-entrant corners on sides of the buildings such as C3, C5, C9, and C11 showed a higher WVR than did the other re-entrant corners because of the aerodynamic effect of the building corners. At α = 67.5°, the WVR in the re-entrant corners of Buildings A and B was lower than that in the re-entrant corners of Buildings C and D because of the wake that developed on the upstream side of Buildings B and C. In C4 and C8, a high WVR was observed. At α = 90°, the WVR was different than that at α = 0°, because of the different building dimensions. In C4 and C13 a high WVR was observed because of the corner effects of Buildings B and D. At α = 90°, upstream re-entrant corners showed a higher WVR than that in the re-entrant corners on the downstream sides. A summary of the data for the re-entrant corners in the low, moderate, and high wind speed regions is provided in Table 3. At α = 45° and 67.5°, few sensors indicated a low WVR. Furthermore, it was observed that a normal wind direction revealed poor ventilation conditions.

Table 3 Number of sensors in re-entrant corners of Configuration 1

Case 1 (α)	No of sensors			Case 2 (α)	No of sensors			Case 3 (α)	No of sensors		
	L	M	H		L	M	H		L	M	H
0°	6	9	1	**0°**	9	7	**0**	**0°**	4	10	2
22.5°	5	11	0	**22.5°**	3	13	**0**	**22.5°**	3	11	2
45°	1	13	2	**45°**	1	14	**1**	**45°**	0	15	1
67.5°	2	12	2	**67.5°**	1	14	**1**	**67.5°**	1	15	0
90°	6	8	2	**90°**	5	11	**0**	**90°**	4	12	0

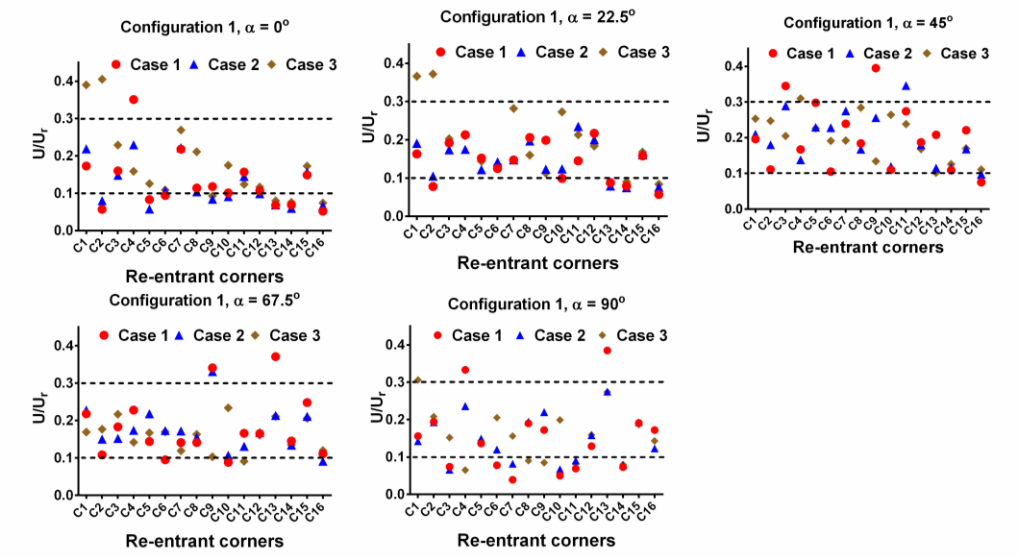

Fig. 6 WVR in various wind incident directions of Configuration 1

3.1.2 Configuration 2

In Configuration 2, nine wind incident directions and 14 re-entrant corners were investigated. Fig. 7 illustrates the WVR distribution in all the re-entrant corners of Configuration 2. At α = 0°, the WVR in the re-entrant corners was higher than that in Configuration 1 because of the removal of Building A, which was in Configuration 1. It was observed that the WVR in the re-entrant corners of the upstream side was more than that on the downstream side. The wind flow behavior through re-entrant corners was similar in Configuration 2 to in Configuration 1. Furthermore, it was noted that in Configuration 2, WVR variations were higher in the re-entrant corners than in Configuration 1. A higher WVR indicates that wind circulation within the re-entrant corners was high and an unstable vortex formed; both of these are suitable for contaminant dispersion and also for natural ventilation. From α = 0° to 90°, limited variation in the WVR was observed except for in few corners. However, from α = 112° to 157.5°, the WVR fluctuation was noted to be higher in most of the re-entrant corners. A summary of the data for the re-entrant corners in three wind

speed regions is provided in Table 4. In this arrangement, α = 45° and 135° indicated a wind environment improved over prior mentioned arrangements. Furthermore, at α = 67.5°, 112.5°, and 157.5°, wind flow improved at a higher degree of building separation.

Table 4 Number of sensors in re-entrant corners of Configuration 2

Case 1 (α)	No of sensors			Case 2 (α)	No of sensors			Case 3 (α)	No of sensors		
	L	M	H		L	M	H		L	M	H
0°	4	10	0	**0°**	4	10	0	**0°**	4	9	1
22.5°	4	9	1	**22.5°**	5	9	0	**22.5°**	3	11	0
45°	1	11	2	**45°**	0	13	1	**45°**	1	13	0
67.5°	2	10	2	**67.5°**	2	11	1	**67.5°**	2	12	0
90°	6	6	2	**90°**	5	9	0	**90°**	5	9	0
112.5°	3	10	1	**112.5°**	2	11	1	**112.5°**	2	11	1
135°	1	10	3	**135°**	1	11	2	**135°**	1	9	4
157.5°	3	11	0	**157.5°**	2	12	0	**157.5°**	2	11	1
180°	6	7	1	**180°**	7	7	0	**180°**	4	10	0

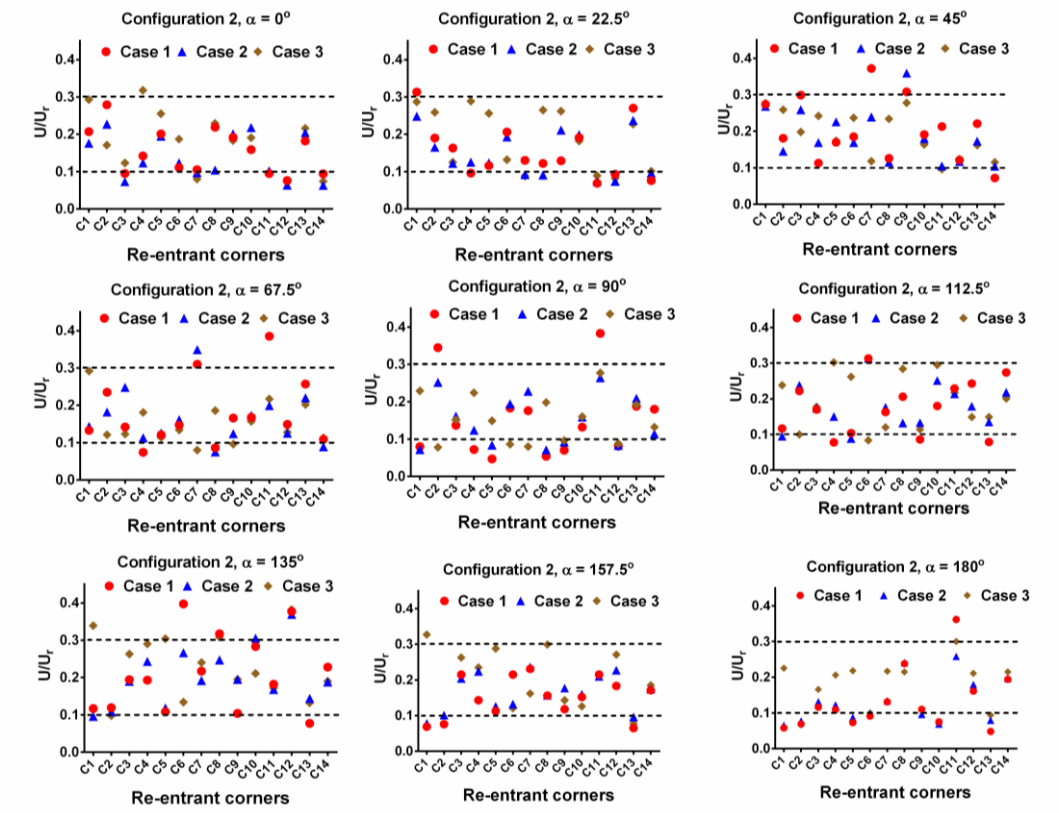

Fig. 7 WVR in various wind incident directions of Configuration 2

3.1.3 Configuration 3

In Configuration 3, 11 wind incident directions and 14 re-entrant corners were investigated. Fig. 8 shows the WVR distribution in the re-entrant corners of Configuration 3. It was observed that in Configuration 3, the WVR distributions were quite similar to those in Configuration 2. However, WVR variations in re-entrant corners were limited compared with those in Configuration 2. In Case 1 and 2, the trend of WVR variations was quite similar. In Case 3, the WVR was different than that in Case 1 and 2. Table 5 presents a summary of the re-entrant corners in three wind speed regions. At $\alpha = 135°$, only one re-entrant corner was observed in low wind speed region. In Case 1, at $\alpha = 90°$, 180°, and 315°, the maximum number of re-entrant corners were observed in low wind speed regions. In these corners, the low WVR was due to the downward wake region and building drag. However, in Case 2 and 3, the WVR was improved because of the increase in passage width and increase in circulation within or proximal to the building corners.

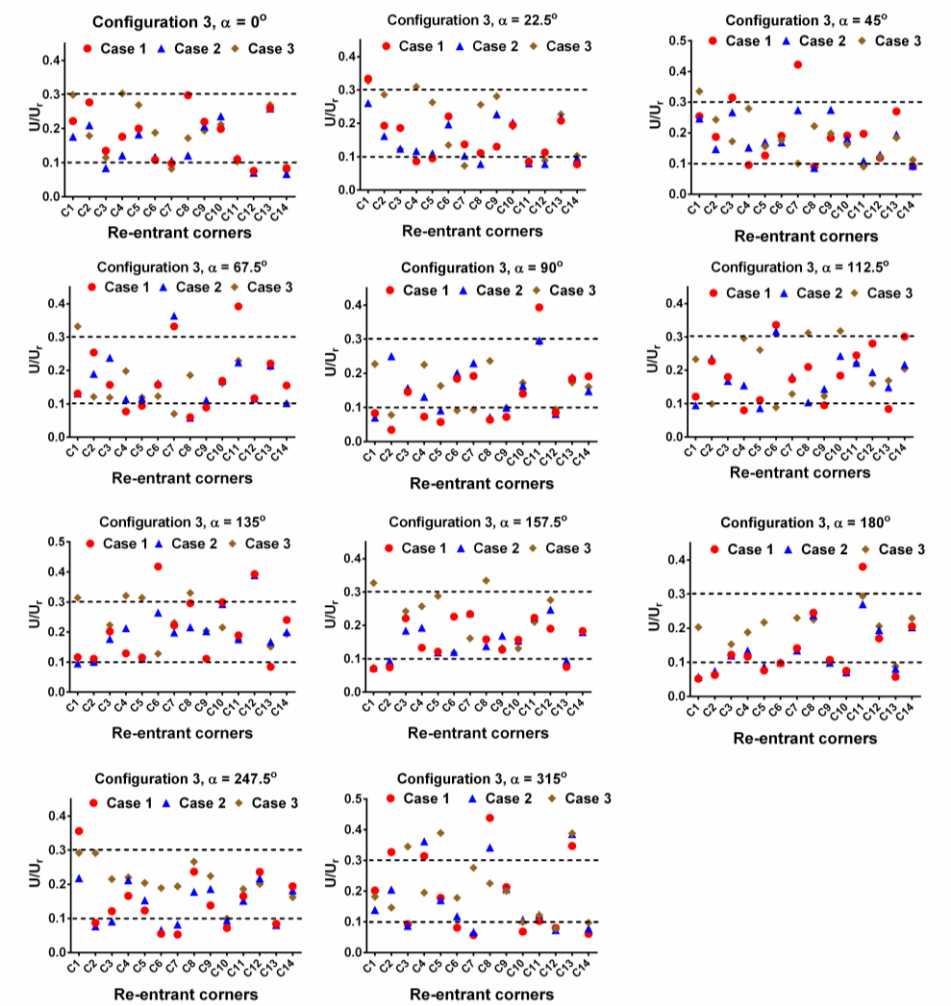

Fig. 8 WVR in various wind incident directions of Configuration 3

Table 5 Number of sensors in re-entrant corners of Configuration 3

Case 1 (α)	No of sensors			Case 2 (α)	No of sensors			Case 3 (α)	No of sensors		
	L	M	H		L	M	H		L	M	H
0°	3	11	0	**0°**	3	11	0	**0°**	3	10	1
22.5°	4	9	1	**22.5°**	4	10	0	**22.5°**	3	9	2
45°	3	9	2	**45°**	2	12	0	**45°**	2	11	1
67.5°	4	8	2	**67.5°**	1	12	1	**67.5°**	1	12	1
90°	6	6	2	**90°**	5	9	0	**90°**	5	9	0
112.5°	3	9	2	**112.5°**	2	11	1	**112.5°**	2	10	2
135°	1	11	2	**135°**	1	12	1	**135°**	1	8	5
157.5°	3	11	0	**157.5°**	3	11	0	**157.5°**	2	10	2
180°	6	7	1	**180°**	7	7	0	**180°**	4	10	0
247.5°	5	8	1	**247.5°**	6	8	0	**247.5°**	2	12	0
315°	6	5	3	**315°**	4	8	2	**315°**	3	8	3

3.1.4 Configuration 4

Fig. 9 illustrates the WVR distribution of Configuration 4, in which five wind directions and 12 re-entrant corners were investigated. At α = 0°, the WVR in C1 and C2 was more than that in the other re-entrant corners. All other re-entrant corners were on the downstream side and showed a low WVR. Similarly, at α = 90°, C2 and C11 were at the end of both sides of the arrangement, and a higher WVR was found in these corners. Upstream and downstream re-entrant corner positions changed with respect to the wind incident direction. In Case 3 of Configuration 4, WVR variations were similar to the other configurations. Table 6 presents a summary of the re-entrant corners. At α = 45°, few re-entrant corners were found in low wind speed regions. At α = 67.5°, wind conditions improved at a higher degree of building separation

3.2 Flow through passages

The influence of wind incident angle on the WVR through passages of case study arrangements is investigated in this section.

Table 6 Number of sensors in re-entrant corners of Configuration 4

Case 1 (α)	No of sensors			Case 2 (α)	No of sensors			Case 3 (α)	No of sensors		
	L	M	H		L	M	H		L	M	H
0°	4	8	0	**0°**	3	9	0	**0°**	1	7	4
22.5°	5	5	2	**22.5°**	3	8	1	**22.5°**	2	10	0
45°	2	8	2	**45°**	2	8	2	**45°**	0	10	2
67.5°	3	7	2	**67.5°**	2	8	2	**67.5°**	0	8	4
90°	6	4	2	**90°**	5	6	1	**90°**	1	9	2

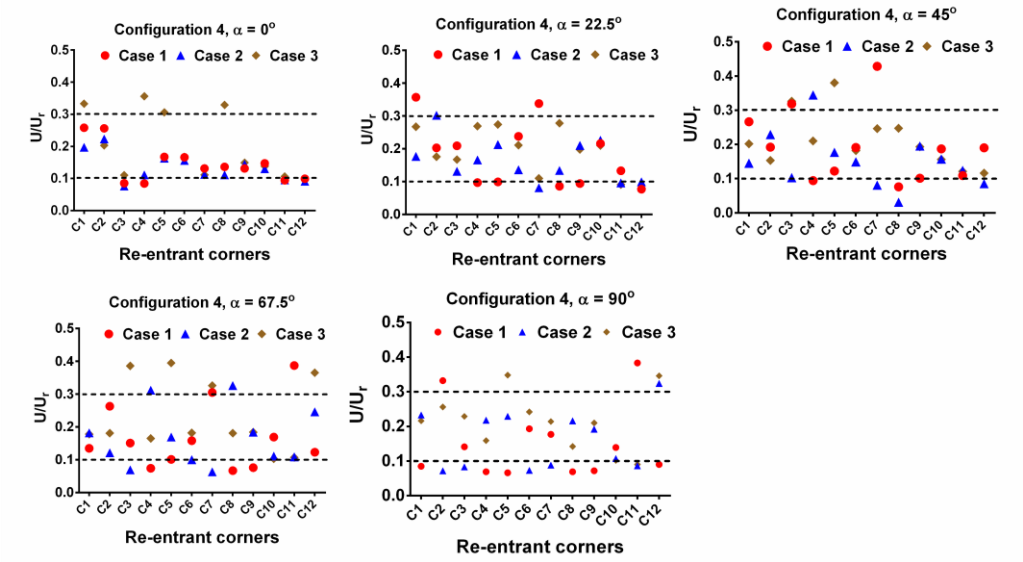

Fig. 9 WVR in various wind incident directions of Configuration 4

3.2.1 Configuration 1

In Configuration 1, flow through four passages was evaluated. The passage positions are provided in Fig. 4. Fig. 10 presents comparisons of the flow through passages. A summary of sensors is provided in Table 7. In Case 1, from α = 0° to 90°, an inverse relation was found between P1 and P4. At α = 45°, in all passages, the WVR was similar, except for a minor change observed in P4. Similarly, at α = 22.5° in P1, the WVR was high because of directly facing the wind, but in P2 to P4, the WVR decreased to the moderate level because of the downstream building wake. Similarly, at α = 67.5°, the WVR in P1 and P4 was reduced by the building wake. In Case 2, WVR variations were similar to Case 1. However, differences in the WVR were reduced because of an increase in passage width. In Case 1, the WVR was high in upstream passages because of the aerodynamic effects of the building corners and passages. In Case 3, passage width increased and venturi effect decreased resulting in a stable flow. In Case 3, for all wind incident directions, most of the passages indicated being a moderate wind speed region. However, in Case 1 and 2, at α = 45° and 67.5°, high wind speed was noted in the passages because of building corners.

3.2.2 Configuration 2

Fig. 11 illustrates the WVR distribution in passages of Configuration 2. The trend of WVR variations was similar to that of Configuration 1. A summary of data for passage sensors is provided in Table 8. The WVR through P1 and P3 changed inversely in all cases with the change in wind incident direction. At α = 45° to 135°, a higher WVR was observed in all cases with respect to the other wind incident angles. However, the overall WVR and the difference in WVR of all passages were reduced from Case 1 to 3. In Case 3, the WVR was lower than that in Case 1 and 2.

Table 7 Number of sensors in passages of Configuration 1

Case 1 (α)	No of sensors			Case 2 (α)	No of sensors			Case 3 (α)	No of sensors		
	L	M	H		L	M	H		L	M	H
0°	0	3	1	**0°**	0	3	1	**0°**	0	3	1
22.5°	0	2	2	**22.5°**	0	1	3	**22.5°**	0	3	1
45°	0	0	4	**45°**	0	0	4	**45°**	0	3	1
67.5°	0	2	2	**67.5°**	0	0	4	**67.5°**	0	2	2
90°	0	2	2	**90°**	0	2	2	**90°**	0	2	2

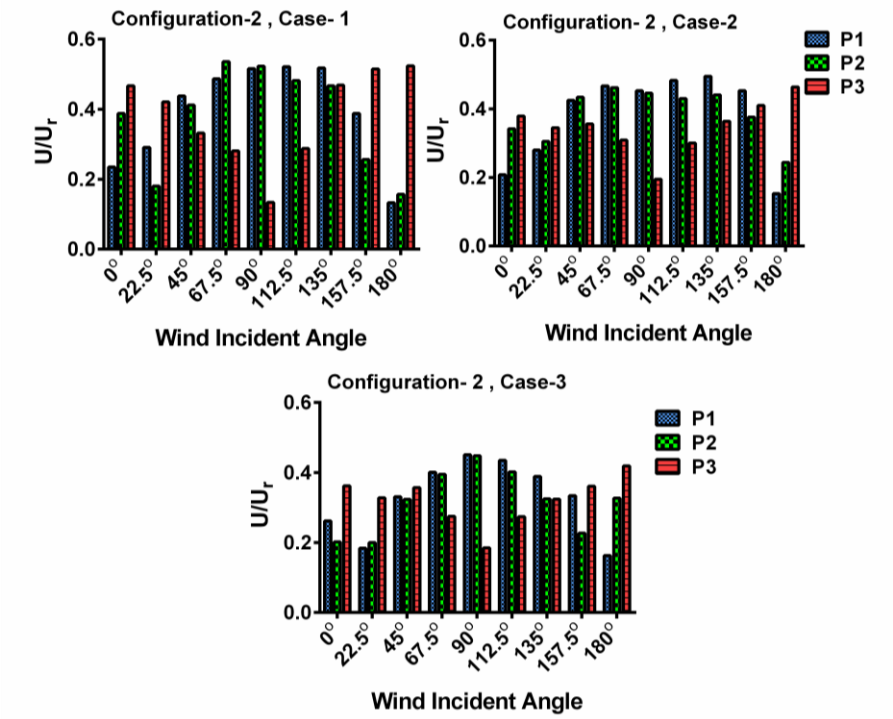

Fig. 11 WVR in passages (P1—P4) of Configuration 2

3.2.3 Configuration 3

Fig. 12 shows the WVR distribution of the Configuration 3 passages. A summary of passage sensors is provided in Table 9. It was noted that in Configuration 3, the overall WVR in all passages was lower than that in Configurations 1 and 2. This was because of the open sides of the building arrangement. At α = 315°, less of a difference in the WVR of passages was observed in all cases because of the symmetrical arrangements of the buildings. Case 3 in Configurations 1 and 2 shows improved results. However, in Configuration 3, the WVR varies with the wind incident directions (Fig. 12).

Table 8 Number of sensors in passages of Configuration 2

Case 1 (α)	No of sensors			Case 2 (α)	No of sensors			Case 3 (α)	No of sensors		
	L	M	H		L	M	H		L	M	H
0°	0	1	2	**0°**	0	1	2	**0°**	0	2	1
22.5°	0	2	1	**22.5°**	0	1	2	**22.5°**	0	2	1
45°	0	0	3	**45°**	0	0	3	**45°**	0	0	3
67.5°	0	1	2	**67.5°**	0	0	3	**67.5°**	0	1	2
90°	0	1	2	**90°**	0	1	2	**90°**	0	1	2
112.5°	0	1	2	**112.5°**	0	1	2	**112.5°**	0	1	2
135°	0	0	3	**135°**	0	0	3	**135°**	0	0	3
157.5°	0	2	1	**157.5°**	0	0	3	**157.5°**	0	1	2
180°	0	2	1	**180°**	0	2	1	**180°**	0	1	2

Table 9 Number of sensors in passages of Configuration 3

Case 1 (α)	No of sensors			Case 2 (α)	No of sensors			Case 3 (α)	No of sensors		
	L	M	H		L	M	H		L	M	H
0°	0	0	3	**0°**	0	1	2	**0°**	0	2	1
22.5°	0	1	2	**22.5°**	0	1	2	**22.5°**	0	2	1
45°	0	1	2	**45°**	0	0	3	**45°**	0	0	3
67.5°	0	1	2	**67.5°**	0	1	2	**67.5°**	0	1	2
90°	0	1	2	**90°**	0	1	2	**90°**	0	1	2
112.5°	0	0	3	**112.5°**	0	0	3	**112.5°**	0	1	2
135°	0	0	3	**135°**	0	0	3	**135°**	0	0	3
157.5°	0	0	3	**157.5°**	0	0	3	**157.5°**	0	1	2
180°	0	2	1	**180°**	0	2	1	**180°**	0	1	2
247.5°	0	2	1	**247.5°**	0	0	3	**247.5°**	0	3	0
315°	0	0	3	**315°**	0	0	3	**315°**	0	2	1

Table 10 Number of sensors in passages of Configuration 4

Case 1 (α)	No of sensors			Case 2 (α)	No of sensors			Case 3 (α)	No of sensors		
	L	M	H		L	M	H		L	M	H
0°	0	2	0	**0°**	0	2	0	**0°**	0	2	0
22.5°	0	0	2	**22.5°**	0	0	2	**22.5°**	0	2	0
45°	0	0	2	**45°**	0	0	2	**45°**	0	2	0
67.5°	0	0	2	**67.5°**	0	0	2	**67.5°**	0	2	0
90°	0	0	2	**90°**	0	0	2	**90°**	0	2	0

3.2.4 Configuration 4

Fig. 13 shows comparisons of the WVR of Configuration 4. A summary of the data for sensors in passages in various WVR regions is provided in Table 10. In Configuration 4, the trends of WVR variations were similar to those in Configuration 1. However, in Case 3 sudden reductions from Case 1 in the WVR were observed. This was because of the absence of the downstream building and an increase in passage width. Table 10 shows that in Case 3 all sensors are in moderate WVR regions.

3.3 Statistical analysis

This section discusses the distribution of WVR by using boxplot in the re-entrant corners of the aforementioned building arrangements..

3.3.1 Configuration 1

Fig. 14 illustrates a box chart of the WVR distribution of Configuration 1. In Case 1 at $\alpha = 45°$, overall WVR variations were higher in all re-entrant corners than those at other wind incident angles. At $\alpha = 90°$, the minimum value of the WVR was lower than 0°; however, a positive Skewness indicated that more re-entrant corners showed a higher WVR than that at 0°. At $\alpha = 67.5°$, a negative Skewness indicated that most of the re-entrant corners showed a low WVR. In Case 2, similar WVR distributions to Case 1 were found. In Case 3, the WVR distribution at $\alpha = 45°$ was symmetrical; however, the WVR at $\alpha = 0°$ was negatively skewed and most of the re-entrant corners showed a low WVR.

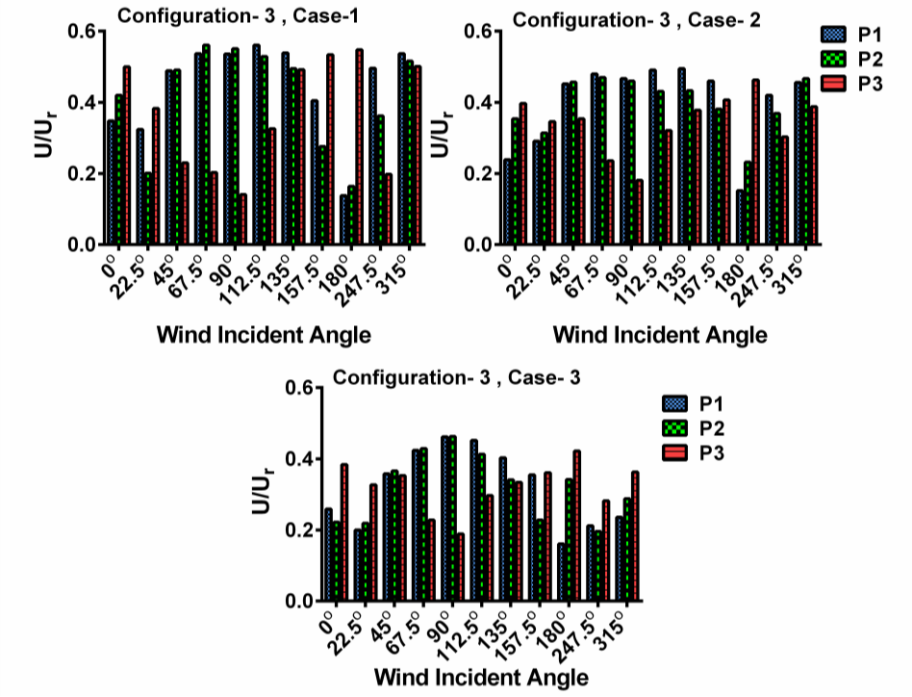

Fig. 12 WVR in passages (P1—P4) of Configuration 3

3.3.2 Configuration 2

Fig. 15 presents a box chart of the WVR distributions of Configuration 2 for all wind incident directions. In Case 1, at $\alpha = 45°$ and 135° a high WVR was observed. At $\alpha = 0°$ in Case 1, the WVR distribution was symmetrical. However, in Case 2 and 3, the WVR was negatively and positively skewed, respectively. This indicates that in Case 2 most of the re-entrant corners had a low WVR. Conversely, in Case 3 most of the re-entrant corners had a higher WVR value. It was observed that in Case 3, all distributions were positively skewed, except at $\alpha = 67.5°$.

3.3.3 Configuration 3

Fig. 16 illustrates a box chart of Configuration 3. In this configuration, the WVR distribution was quite similar to that of Configuration 2. At $\alpha = 315°$, in Case 1 the WVR distribution was negatively skewed. In Case 2, the median moved upwards and showed a slightly higher WVR in some re-entrant corners. In Case 3, the WVR distributions became symmetrical. This indicates that passage width plays a critical role in wind flow through re-entrant corners. Similar to Configuration 2, in Case 3 all the WVR distribution was symmetrical or positively skewed, except at $\alpha = 67.5°$.

3.3.4 Configuration 4

In Case 1 of Configuration 4, the WVR distribution was similar to that of Configuration 1. However, in Configuration 4 the WVR was higher than that in Configuration 1. Fig. 17 illustrates the boxplot of Configuration 4. It was observed that from Case 1 to 3, the distribution of WVR in a downstream corners increased at $\alpha = 0°$, 45°, and 67.5°. This is because of the inherent seclusion of the building within the downstream wake region.

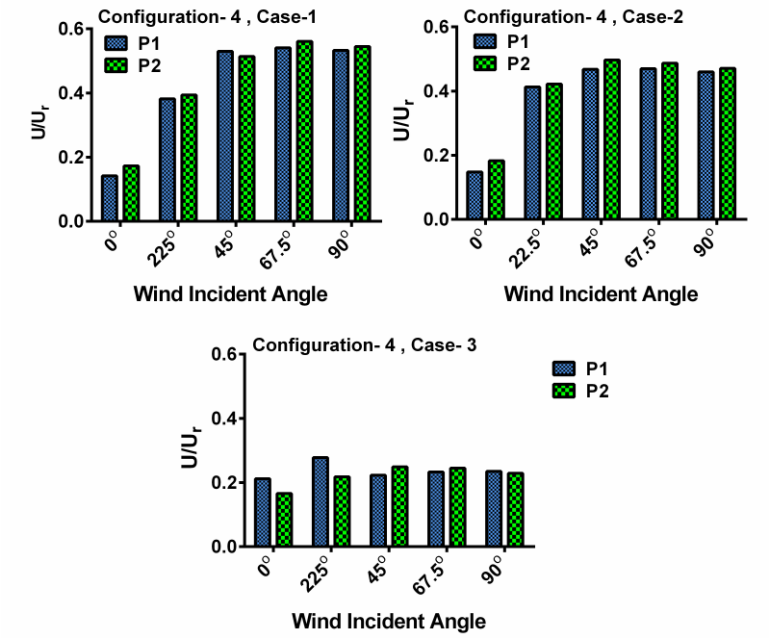

Fig. 13 WVR in passages (P1—P4) of Configuration 4

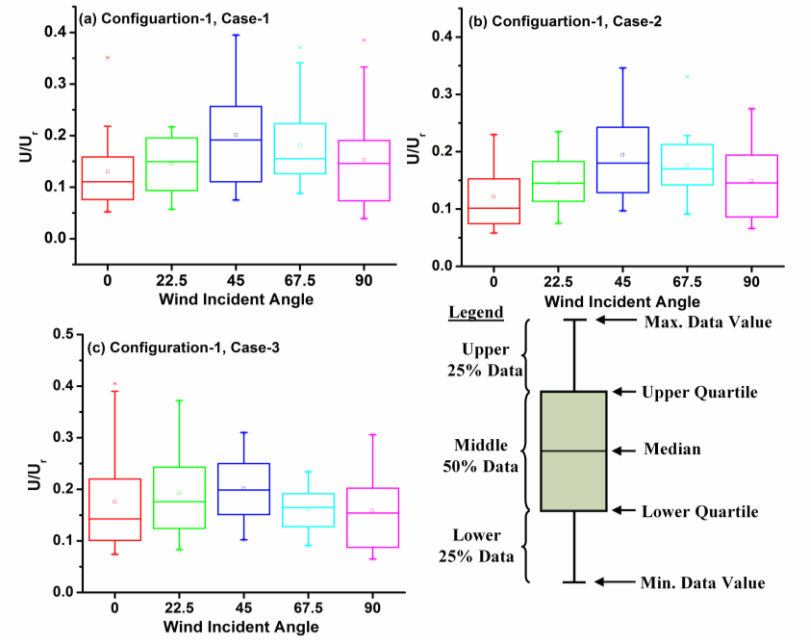

Fig. 14 Boxplot of the mean WVR in re-entrant corners of Configuration 1

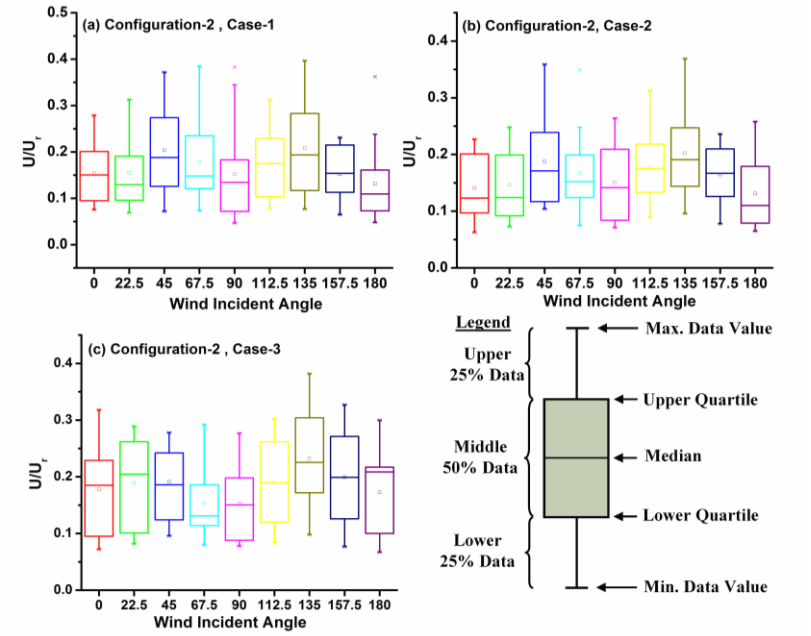

Fig. 15 Boxplot of the mean WVR in re-entrant corners of Configuration 2

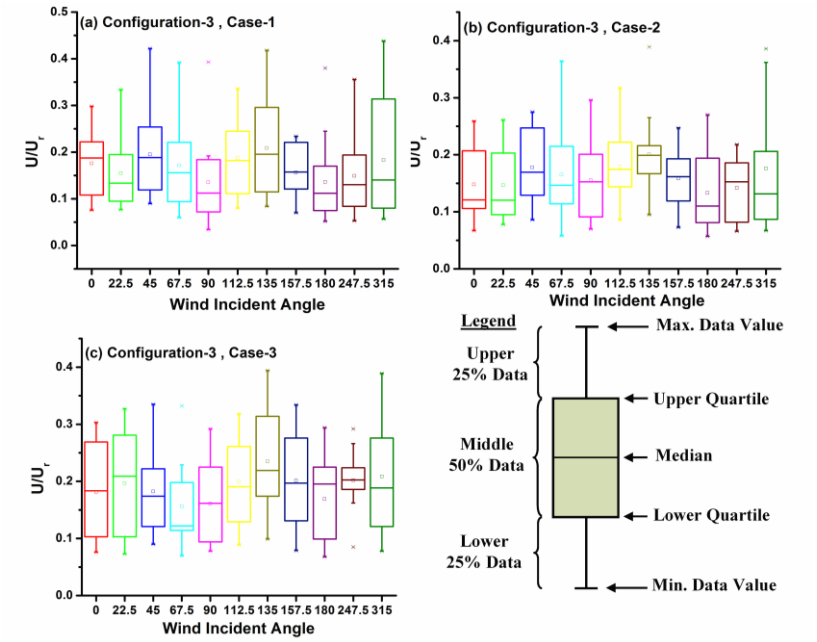

Fig. 16 Boxplot of the mean WVR in re-entrant corners of Configuration 3

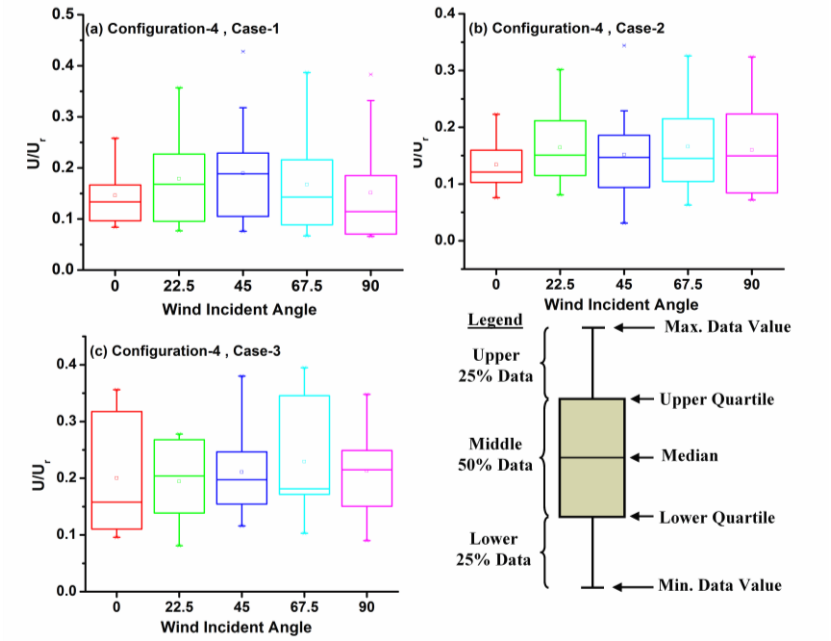

Fig. 17 Boxplot of the mean WVR in re-entrant corners of Configuration 4

4. Conclusions

This study investigated wind circulation in the re-entrant corners from various wind incident directions. The results show that oblique orientations of buildings improve the wind flow in the re-entrant corners. In oblique wind incident directions, wind circulation increases within the re-entrant corners because of the aerodynamic effects of square corners. High circulation destabilizes the vortices and increases the swirl flow and ultimately increases the wind flow rate in the re-entrant corners and passages. Furthermore, it was observed that wind incident angles close to 45°, 135°, and 315° showed positive results. From wind incident angle of 0° to 90° (at W=0.142m in configuration 1), highest number (78.75%) of the re-entrant corners was in moderate wind speed region. Similarly, at wind incident angle ranging from 0° to 180°, at W=0.142 m and 0.107 m, configuration 2 and 3 exhibited highest number (75.4%) of the re-entrant corners in the moderate wind speed region, respectively. Overall, L-shaped buildings arrangement exhibited the highest wind circulation in the re-entrant corners that was based on the lower and greater number of re-entrant corners in the low and moderate wind speed regions, respectively.

In a second step, wind flow through passages was examined. In passages, a high normalized wind speed was observed at W=0.054m. However, in all configurations, at W=0.142 m, normalized wind speed was reduced because of an increase in building separation. Furthermore, the results show that wind circulation in the re-entrant corners and passages can be improved by oblique wind direction and appropriate building separation. Moreover, statistical analysis indicated that wind incident angles of 45°, 135°, and 315° provided a wide distribution of normalized wind speed and were suitable for enhanced wind flow within the re-entrant corners and around the buildings. In future, pollutant source will be used in "the re-entrant corners to investigate the influence of wind directions on pollution dispersion.

Acknowledgments

This study was supported by a postgraduate studentship award from the City University of Hong Kong. Special thanks are extended to the support staff of the wind tunnel lab. The anonymous reviewers who provided constructive comments are also gratefully acknowledged.

References

Afiq W.M.Y., Azwadi C.S.N. and Saqr, K.M. (2012), "Effects of buildings aspect ratio, wind speed and wind direcion on flow structure and pollutant dispersion in symmetric street canyons: A review", *Int. J. Mech. Mater. Eng*., **7**(2),158-165.

Blocken, B. andCarmeliet, J. (2004), "Pedestrian wind environment around buildings: Literature review and practical examples", *J. Build.Phys*., **28**(2),107-159.

Blocken, B. and Stathopoulos, T. (2013), "CFD simulation of pedestrian-level wind conditions around buildings: Past achievements and prospects", *J. Wind Eng. Ind. Aerod*., **121**, 138-145.

Blocken, B. (2014), "50 years of computational wind engineering: Past, present and future", *J. Wind Eng. Ind. Aerod*., **129**, 69-102. Retrieved November 3, 2014.

Blocken, B. (2015), "Computational fluid dynamics for urban physics: Importance, scales, possibilities, limitations and ten tips and tricks towards accurate and reliable simulations", *Build. Environ*., **91**, 219-245.

Cheng, C.K.C., Lam, K.M., Leung, Y.T.A., Yang, K., Danny, H.W.L. and Sherman, C.P.C. (2011), "Wind-induced natural ventilation of re-entrant bays in a high-rise building", *J. Wind Eng. Ind. Aerod*., **99**(2-3),79-90.

Chow, T.T., Lin, Z. and Liu, J.P. (2002), "Effect of condensing unit layout at building re-entrant on split-type air-conditioner performance", *Architect. Sci. Rev*., **45**(1), 3-11.

Franke, J., Antti Hellsten, H.S. and Bertrand, C. (2007), *Best Practice Guideline for the CFD Simulation of Flows in the Urban Environment*.

Gao, N.P., Niu, J.L., Perino, M. and Heiselberg., P. (2009), "The airborne transmission of infection between flats in high-rise residential buildings: Tracer gas simulation", *Build. Environmen*, **44**, 402-410.

Gomes, M.G., Rodrigues, A.M. and Mendes, P. (2005), "Experimental and numerical study of wind pressures on irregular-plan shapes", *J. Wind Eng. Ind. Aerod*., **93**(10), 741-756.

Hang, J., Li, Y., Sandberg, M., Buccolieri, R. and Sabatino, S.D. (2012), "The influence of building height variability on pollutant dispersion and pedestrian ventilation in idealized high-rise urban areas", *Build. Environ.*, **56**, 346-360.

Higson, H.L., Griffiths, R.F., Jones, C.D. and Hall, D.J. (1996), "Flow and dispersion around an isolated building", *Atmosph. Environ*., **30**(16), 2859-2870.

Janssen, W.D., Blocken, B. and van Hooff, T. (2013), "Pedestrian wind comfort around buildings: Comparison of wind comfort criteria based on whole-flow field data for a complex case study", *Build. Environment*, **59**, 547-562.

Kubota, T., Miura, M., Tominaga, Y. and Mochida, A. (2008), "Wind tunnel tests on the relationship between building density and pedestrian-level wind velocity: Development of guidelines for realizing acceptable wind environment in residential neighborhoods", *Build. Environ.*, **43**(10), 1699-1708.

Ng, E. (2009), "Policies and technical guidelines for urban planning of high-density cities - Air Ventilation Assessment (AVA) of Hong Kong", *Build. Environ.*, **44**(7), 1478-1488.

Santos, J.M., Griffiths, R.F., Roberts, I.D. and Reis, N.C. (2005), "A field experiment on turbulent concentration fluctuations of an atmospheric tracer gas in the vicinity of a complex-shaped building", *Atmos. Environ*., **39**(28), 4999-5012.

Snyder, W.H. (1972), "Similarity criteria for the application of fluid models to the study of air pollution meteorology", *Bound. - Lay. Meteorol.*, **3**, 113-134.

Stathopoulos, T., Wu, H. and Bédard, C. (1992), "Wind environment around buildings: A knowledge-based approach", *J. Wind Eng. Ind. Aerod.*, **44**(1-3), 2377-2388.

Stathopoulos, T. (2006), "Pedestrian level winds and outdoor human comfort", *J. Wind Eng. Ind. Aerod*., **94**(11), 769-780.

Tominaga, Y., Mochida, A., Yoshie, R., Kataoka, H., Nozu, T., Yoshikawa, M. and Shirasawa, T. (2008), "AIJ guidelines for practical applications of CFD to pedestrian wind environment around buildings", *J. Wind Eng. Ind. Aerod*., **96**(10-11), 1749-1761.

Tsang, C.W., Kwok, K.C.S. and Hitchcock, P.A. (2012), "Wind tunnel study of pedestrian level wind environment around tall buildings: Effects of building dimensions, separation and podium", *Build. Environ.*, **49**, 167-181.

Wang, Y., Zhou, Y. Zhu, Y. and Tse Tim, K.T. (2012), "Numerical prediction of wind flow around irregular models", *J. Fluids Eng*., **134**(7), 071108.

Wong, S.Y. and Lam, K.M. (2013), "Effect of recessed cavities on wind-induced loading and dynamic responses of a tall building", *J. Wind Eng. Ind. Aerod*., **114**, 72-82.

Yang, F., Kang, Y., Gao, Y. and Zhong, K. (2015), "Numerical simulations of the effect of outdoor pollutants on indoor air quality of buildings next to a street canyon", *Build. Environ.*, **87**, 10-22.

Yeung, K.H., and Yu, I.T.S. (2007), "Possible meteorological influence on the Severe Acute Respiratory Syndrome (SARS) community outbreak at amoy gardens,Hong Kong", *J. Environ. Health*, **70**(3), 39-46.

Zhang, Y., Kwok, K.C.S., Liu, X.P. and Niu, J.L. (2015), "Characteristics of air pollutant dispersion around a high-rise building", *Environmental pollution (Barking, Essex : 1987)*, **204**, 280-288.

CC